



## UvA-DARE (Digital Academic Repository)

### Search for $\gamma$ -Ray Line Signals from Dark Matter Annihilations in the Inner Galactic Halo from 10 Years of Observations with H.E.S.S.

Abdallah, H.; Balzer, A.; Berge, D.; Bryan, M.; Edwards, T.; Prokoph, H.; Simoni, R.; Vink, J.; H.E.S.S. Collaboration

**DOI**

[10.1103/PhysRevLett.120.201101](https://doi.org/10.1103/PhysRevLett.120.201101)

**Publication date**

2018

**Document Version**

Final published version

**Published in**

Physical Review Letters

[Link to publication](#)

**Citation for published version (APA):**

Abdallah, H., Balzer, A., Berge, D., Bryan, M., Edwards, T., Prokoph, H., Simoni, R., Vink, J., & H.E.S.S. Collaboration (2018). Search for  $\gamma$  -Ray Line Signals from Dark Matter Annihilations in the Inner Galactic Halo from 10 Years of Observations with H.E.S.S. *Physical Review Letters*, 120(20), Article 201101. <https://doi.org/10.1103/PhysRevLett.120.201101>

**General rights**

It is not permitted to download or to forward/distribute the text or part of it without the consent of the author(s) and/or copyright holder(s), other than for strictly personal, individual use, unless the work is under an open content license (like Creative Commons).

**Disclaimer/Complaints regulations**

If you believe that digital publication of certain material infringes any of your rights or (privacy) interests, please let the Library know, stating your reasons. In case of a legitimate complaint, the Library will make the material inaccessible and/or remove it from the website. Please Ask the Library: <https://uba.uva.nl/en/contact>, or a letter to: Library of the University of Amsterdam, Secretariat, Singel 425, 1012 WP Amsterdam, The Netherlands. You will be contacted as soon as possible.

*UvA-DARE is a service provided by the library of the University of Amsterdam (<https://dare.uva.nl>)*

## Search for $\gamma$ -Ray Line Signals from Dark Matter Annihilations in the Inner Galactic Halo from 10 Years of Observations with H.E.S.S.

H. Abdallah,<sup>1</sup> A. Abramowski,<sup>2</sup> F. Aharonian,<sup>3,4,5</sup> F. Ait Benkhali,<sup>3</sup> E. O. Angüner,<sup>6</sup> M. Arakawa,<sup>7</sup> M. Arrieta,<sup>8</sup> P. Aubert,<sup>9</sup> M. Backes,<sup>10</sup> A. Balzer,<sup>11</sup> M. Barnard,<sup>1</sup> Y. Becherini,<sup>12</sup> J. Becker Tjus,<sup>13</sup> D. Berge,<sup>11</sup> S. Bernhard,<sup>14</sup> K. Bernlöhr,<sup>3</sup> R. Blackwell,<sup>15</sup> M. Böttcher,<sup>1</sup> C. Boisson,<sup>8</sup> J. Bolmont,<sup>16</sup> S. Bonnefoy,<sup>17</sup> P. Bordas,<sup>3</sup> J. Bregeon,<sup>18</sup> F. Brun,<sup>19</sup> P. Brun,<sup>20</sup> M. Bryan,<sup>11</sup> M. Büchele,<sup>21</sup> T. Bulik,<sup>22</sup> M. Capasso,<sup>23</sup> S. Caroff,<sup>24</sup> A. Carosi,<sup>9</sup> J. Carr,<sup>25</sup> S. Casanova,<sup>6,3</sup> M. Cerruti,<sup>16</sup> N. Chakraborty,<sup>3</sup> R. C. G. Chaves,<sup>18</sup> A. Chen,<sup>26</sup> J. Chevalier,<sup>9</sup> S. Colafrancesco,<sup>26</sup> B. Condon,<sup>19</sup> J. Conrad,<sup>27</sup> I. D. Davids,<sup>10</sup> J. Decock,<sup>20</sup> C. Deil,<sup>3</sup> J. Devin,<sup>18</sup> P. deWilt,<sup>15</sup> L. Dirson,<sup>2</sup> A. Djannati-Ataï,<sup>28</sup> W. Domainko,<sup>3</sup> A. Donath,<sup>3</sup> L. O'C. Drury,<sup>4</sup> K. Dutson,<sup>29</sup> J. Dyks,<sup>30</sup> T. Edwards,<sup>3</sup> K. Egberts,<sup>31</sup> P. Eger,<sup>3</sup> G. Emery,<sup>16</sup> J.-P. Ernenwein,<sup>25</sup> S. Eschbach,<sup>21</sup> C. Farnier,<sup>27,12</sup> S. Fegan,<sup>24</sup> M. V. Fernandes,<sup>2</sup> A. Fiasson,<sup>9</sup> G. Fontaine,<sup>24</sup> A. Förster,<sup>3</sup> S. Funk,<sup>21</sup> M. Füßling,<sup>17</sup> S. Gabici,<sup>28</sup> Y. A. Gallant,<sup>18</sup> T. Garrigoux,<sup>1</sup> F. Gaté,<sup>9</sup> G. Giavitto,<sup>17</sup> B. Giebels,<sup>24</sup> D. Glawion,<sup>32</sup> J. F. Glicenstein,<sup>20</sup> D. Gottschall,<sup>23</sup> M.-H. Grondin,<sup>19</sup> J. Hahn,<sup>3</sup> M. Haupt,<sup>17</sup> J. Hawkes,<sup>15</sup> G. Heinzlmann,<sup>2</sup> G. Henri,<sup>33</sup> G. Hermann,<sup>3</sup> J. A. Hinton,<sup>3</sup> W. Hofmann,<sup>3</sup> C. Hoischen,<sup>31</sup> T. L. Holch,<sup>34</sup> M. Holler,<sup>14</sup> D. Horns,<sup>2</sup> A. Ivascenko,<sup>1</sup> H. Iwasaki,<sup>7</sup> A. Jacholkowska,<sup>16</sup> M. Jamrozny,<sup>35</sup> M. Janiak,<sup>30</sup> D. Jankowsky,<sup>21</sup> F. Jankowsky,<sup>32</sup> M. Jingo,<sup>26</sup> L. Jouvin,<sup>28</sup> I. Jung-Richardt,<sup>21</sup> M. A. Kastendieck,<sup>2</sup> K. Katarzyński,<sup>36</sup> M. Katsuragawa,<sup>37</sup> U. Katz,<sup>21</sup> D. Kerszberg,<sup>16</sup> D. Khangulyan,<sup>7</sup> B. Khélifi,<sup>28</sup> J. King,<sup>3</sup> S. Klepser,<sup>17</sup> D. Klochkov,<sup>23</sup> W. Kluźniak,<sup>30</sup> Nu. Komin,<sup>26</sup> K. Kosack,<sup>20</sup> S. Krakau,<sup>13</sup> M. Kraus,<sup>21</sup> P. P. Krüger,<sup>1</sup> H. Laffon,<sup>19</sup> G. Lamanna,<sup>9</sup> J. Lau,<sup>15</sup> J.-P. Lees,<sup>9</sup> J. Lefaucheur,<sup>8</sup> A. Lemièrre,<sup>28</sup> M. Lemoine-Goumard,<sup>19</sup> J.-P. Lenain,<sup>16</sup> E. Leser,<sup>31</sup> R. Liu,<sup>3</sup> T. Lohse,<sup>34</sup> M. Lorentz,<sup>20</sup> R. López-Coto,<sup>3</sup> I. Lypova,<sup>17</sup> D. Malyshev,<sup>23</sup> V. Marandon,<sup>3</sup> A. Marcowith,<sup>18</sup> C. Mariaud,<sup>24</sup> R. Marx,<sup>3</sup> G. Maurin,<sup>9</sup> N. Macted,<sup>15,\*</sup> M. Mayer,<sup>34</sup> P. J. Meintjes,<sup>38</sup> M. Meyer,<sup>27</sup> A. M. W. Mitchell,<sup>3</sup> R. Moderski,<sup>30</sup> M. Mohamed,<sup>32</sup> L. Mohrmann,<sup>21</sup> K. Morá,<sup>27</sup> E. Moulin,<sup>20,†</sup> T. Murach,<sup>17</sup> S. Nakashima,<sup>37</sup> M. de Naurois,<sup>24</sup> H. Ndiyavala,<sup>1</sup> F. Niederwanger,<sup>14</sup> J. Niemiec,<sup>6</sup> L. Oakes,<sup>34</sup> P. O'Brien,<sup>29</sup> H. Odaka,<sup>37</sup> S. Ohm,<sup>17</sup> M. Ostrowski,<sup>35</sup> I. Oya,<sup>17</sup> M. Padovani,<sup>18</sup> M. Panter,<sup>3</sup> R. D. Parsons,<sup>3</sup> N. W. Pekeur,<sup>1</sup> G. Pelletier,<sup>33</sup> C. Perennes,<sup>16</sup> P.-O. Petrucci,<sup>33</sup> B. Peyaud,<sup>20</sup> Q. Piel,<sup>9</sup> S. Pita,<sup>28</sup> V. Poireau,<sup>9</sup> H. Poon,<sup>3</sup> D. Prokhorov,<sup>12</sup> H. Prokoph,<sup>11</sup> G. Pühlhofer,<sup>23</sup> M. Punch,<sup>28,12</sup> A. Quirrenbach,<sup>32</sup> S. Raab,<sup>21</sup> R. Rauth,<sup>14</sup> A. Reimer,<sup>14</sup> O. Reimer,<sup>14</sup> M. Renaud,<sup>18</sup> R. de los Reyes,<sup>3</sup> F. Rieger,<sup>3</sup> L. Rinchiuso,<sup>20,†</sup> C. Romoli,<sup>4</sup> G. Rowell,<sup>15</sup> B. Rudak,<sup>30</sup> C. B. Rulten,<sup>8</sup> V. Sahakian,<sup>5,39</sup> S. Saito,<sup>7</sup> D. A. Sanchez,<sup>9</sup> A. Santangelo,<sup>23</sup> M. Sasaki,<sup>21</sup> M. Schandri,<sup>21</sup> R. Schlickeiser,<sup>13</sup> F. Schüssler,<sup>20</sup> A. Schulz,<sup>17</sup> U. Schwanke,<sup>34</sup> S. Schwemmer,<sup>32</sup> M. Seglar-Arroyo,<sup>20</sup> M. Settimo,<sup>16</sup> A. S. Seyffert,<sup>1</sup> N. Shafi,<sup>26</sup> I. Shilon,<sup>21</sup> K. Shiningayamwe,<sup>10</sup> R. Simoni,<sup>11</sup> H. Sol,<sup>8</sup> F. Spanier,<sup>1</sup> M. Spir-Jacob,<sup>28</sup> Ł. Stawarz,<sup>35</sup> R. Steenkamp,<sup>10</sup> C. Stegmann,<sup>31,17</sup> C. Steppa,<sup>31</sup> I. Sushch,<sup>1</sup> T. Takahashi,<sup>37</sup> J.-P. Tavernet,<sup>16</sup> T. Tavernier,<sup>28</sup> A. M. Taylor,<sup>17</sup> R. Terrier,<sup>28</sup> L. Tibaldo,<sup>3</sup> D. Tiziani,<sup>21</sup> M. Tluczykont,<sup>2</sup> C. Trichard,<sup>25</sup> M. Tzirou,<sup>18</sup> N. Tsuji,<sup>7</sup> R. Tuffs,<sup>3</sup> Y. Uchiyama,<sup>7</sup> J. van der Walt,<sup>1</sup> C. van Eldik,<sup>21</sup> C. van Rensburg,<sup>1</sup> B. van Soelen,<sup>38</sup> G. Vasileiadis,<sup>18</sup> J. Veh,<sup>21</sup> C. Venter,<sup>1</sup> A. Viana,<sup>3,‡</sup> P. Vincent,<sup>16</sup> J. Vink,<sup>11</sup> F. Voisin,<sup>15</sup> H. J. Völk,<sup>3</sup> T. Vuillaume,<sup>9</sup> Z. Wadiasingh,<sup>1</sup> S. J. Wagner,<sup>32</sup> P. Wagner,<sup>34</sup> R. M. Wagner,<sup>27</sup> R. White,<sup>3</sup> A. Wiercholska,<sup>6</sup> P. Willmann,<sup>21</sup> A. Wörnlein,<sup>21</sup> D. Wouters,<sup>20</sup> R. Yang,<sup>3</sup> D. Zaborov,<sup>24</sup> M. Zacharias,<sup>1</sup> R. Zanin,<sup>3</sup> A. A. Zdziarski,<sup>30</sup> A. Zech,<sup>8</sup> F. Zefi,<sup>24</sup> A. Ziegler,<sup>21</sup> J. Zorn,<sup>3</sup> and N. Żywucka<sup>35</sup>

(H.E.S.S. Collaboration)

<sup>1</sup>Centre for Space Research, North-West University, Potchefstroom 2520, South Africa

<sup>2</sup>Universität Hamburg, Institut für Experimentalphysik, Luruper Chaussee 149, D 22761 Hamburg, Germany

<sup>3</sup>Max-Planck-Institut für Kernphysik, P.O. Box 103980, D 69029 Heidelberg, Germany

<sup>4</sup>Dublin Institute for Advanced Studies, 31 Fitzwilliam Place, Dublin 2, Ireland

<sup>5</sup>National Academy of Sciences of the Republic of Armenia, Marshall Baghramian Avenue, 24, 0019 Yerevan, Armenia

<sup>6</sup>Instytut Fizyki Jądrowej PAN, ul. Radzikowskiego 152, 31-342 Kraków, Poland

<sup>7</sup>Department of Physics, Rikkyo University, 3-34-1 Nishi-Ikebukuro, Toshima-ku, Tokyo 171-8501, Japan

<sup>8</sup>LUTH, Observatoire de Paris, PSL Research University, CNRS, Université Paris Diderot,

5 Place Jules Janssen, 92190 Meudon, France

<sup>9</sup>Laboratoire d'Annecy-le-Vieux de Physique des Particules, Université Savoie Mont-Blanc,

CNRS/IN2P3, F-74941 Annecy-le-Vieux, France

<sup>10</sup>University of Namibia, Department of Physics, Private Bag 13301, Windhoek, Namibia

<sup>11</sup>GRAPPA, Anton Pannekoek Institute for Astronomy and Institute of High-Energy Physics, University of Amsterdam, Science Park 904, 1098 XH Amsterdam, Netherlands

<sup>12</sup>Department of Physics and Electrical Engineering, Linnaeus University, 351 95 Växjö, Sweden

- <sup>13</sup>*Institut für Theoretische Physik, Lehrstuhl IV: Weltraum und Astrophysik, Ruhr-Universität Bochum, D 44780 Bochum, Germany*
- <sup>14</sup>*Institut für Astro- und Teilchenphysik, Leopold-Franzens-Universität Innsbruck, A-6020 Innsbruck, Austria*
- <sup>15</sup>*School of Chemistry and Physics, University of Adelaide, Adelaide 5005, Australia*
- <sup>16</sup>*Sorbonne Universités, UPMC Université Paris 06, Université Paris Diderot, Sorbonne Paris Cité, CNRS, Laboratoire de Physique Nucléaire et de Hautes Energies (LPNHE), 4 place Jussieu, F-75252 Paris Cedex 5, France*
- <sup>17</sup>*DESY, D-15738 Zeuthen, Germany*
- <sup>18</sup>*Laboratoire Univers et Particules de Montpellier, Université Montpellier, CNRS/IN2P3, CC 72, Place Eugène Bataillon, F-34095 Montpellier Cedex 5, France*
- <sup>19</sup>*Université Bordeaux I, CNRS/IN2P3, Centre d'Études Nucléaires de Bordeaux Gradignan, 33175 Gradignan, France*
- <sup>20</sup>*IRFU, CEA, Université Paris-Saclay, F-91191 Gif-sur-Yvette, France*
- <sup>21</sup>*Friedrich-Alexander-Universität Erlangen-Nürnberg, Erlangen Centre for Astroparticle Physics, Erwin-Rommel-Strasse 1, D 91058 Erlangen, Germany*
- <sup>22</sup>*Astronomical Observatory, The University of Warsaw, Al. Ujazdowskie 4, 00-478 Warsaw, Poland*
- <sup>23</sup>*Institut für Astronomie und Astrophysik, Universität Tübingen, Sand 1, D 72076 Tübingen, Germany*
- <sup>24</sup>*Laboratoire Leprince-Ringuet, Ecole Polytechnique, CNRS/IN2P3, F-91128 Palaiseau, France*
- <sup>25</sup>*Aix Marseille Université, CNRS/IN2P3, CPPM UMR 7346, 13288 Marseille, France*
- <sup>26</sup>*School of Physics, University of the Witwatersrand, 1 Jan Smuts Avenue, Braamfontein, Johannesburg, 2050 South Africa*
- <sup>27</sup>*Oskar Klein Centre, Department of Physics, Stockholm University, Albanova University Center, SE-10691 Stockholm, Sweden*
- <sup>28</sup>*APC, AstroParticule et Cosmologie, Université Paris Diderot, CNRS/IN2P3, CEA/Irfu, Observatoire de Paris, Sorbonne Paris Cité, 10, rue Alice Domon et Léonie Duquet, 75205 Paris Cedex 13, France*
- <sup>29</sup>*Department of Physics and Astronomy, The University of Leicester, University Road, Leicester LE1 7RH, United Kingdom*
- <sup>30</sup>*Nicolaus Copernicus Astronomical Center, Polish Academy of Sciences, ul. Bartycka 18, 00-716 Warsaw, Poland*
- <sup>31</sup>*Institut für Physik und Astronomie, Universität Potsdam, Karl-Liebknecht-Strasse 24/25, D 14476 Potsdam, Germany*
- <sup>32</sup>*Landessternwarte, Universität Heidelberg, Königstuhl, D 69117 Heidelberg, Germany*
- <sup>33</sup>*Université Grenoble Alpes, CNRS, IPAG, F-38000 Grenoble, France*
- <sup>34</sup>*Institut für Physik, Humboldt-Universität zu Berlin, Newtonstrasse 15, D 12489 Berlin, Germany*
- <sup>35</sup>*Obserwatorium Astronomiczne, Uniwersytet Jagielloński, ul. Orła 171, 30-244 Kraków, Poland*
- <sup>36</sup>*Centre for Astronomy, Faculty of Physics, Astronomy and Informatics, Nicolaus Copernicus University, Grudziadzka 5, 87-100 Toruń, Poland*
- <sup>37</sup>*Japan Aerospace Exploration Agency (JAXA), Institute of Space and Astronautical Science (ISAS), 3-1-1 Yoshinodai, Chuo-ku, Sagami-hara, Kanagawa 229-8510, Japan*
- <sup>38</sup>*Department of Physics, University of the Free State, P.O. Box 339, Bloemfontein 9300, South Africa*
- <sup>39</sup>*Yerevan Physics Institute, 2 Alikhanian Brothers Street, 375036 Yerevan, Armenia*

 (Received 23 October 2017; revised manuscript received 5 March 2018; published 15 May 2018)

Spectral lines are among the most powerful signatures for dark matter (DM) annihilation searches in very-high-energy  $\gamma$  rays. The central region of the Milky Way halo is one of the most promising targets given its large amount of DM and proximity to Earth. We report on a search for a monoenergetic spectral line from self-annihilations of DM particles in the energy range from 300 GeV to 70 TeV using a two-dimensional maximum likelihood method taking advantage of both the spectral and spatial features of the signal versus background. The analysis makes use of Galactic center observations accumulated over ten years (2004–2014) with the H.E.S.S. array of ground-based Cherenkov telescopes. No significant  $\gamma$ -ray excess above the background is found. We derive upper limits on the annihilation cross section  $\langle\sigma v\rangle$  for monoenergetic DM lines at the level of  $4 \times 10^{-28} \text{ cm}^3 \text{ s}^{-1}$  at 1 TeV, assuming an Einasto DM profile for the Milky Way halo. For a DM mass of 1 TeV, they improve over the previous ones by a factor of 6. The present constraints are the strongest obtained so far for DM particles in the mass range 300 GeV–70 TeV. Ground-based  $\gamma$ -ray observations have reached sufficient sensitivity to explore relevant velocity-averaged cross sections for DM annihilation into two  $\gamma$ -ray photons at the level expected from the thermal relic density for TeV DM particles.

DOI: [10.1103/PhysRevLett.120.201101](https://doi.org/10.1103/PhysRevLett.120.201101)

*Introduction.*—Cosmological measurements show that about 85% of the matter in the Universe is nonbaryonic cold dark matter (DM) [1]. A leading class of DM particle candidates consists of weakly interacting massive particles (WIMPs) [2–5]. Thermally produced in the early Universe, stable particles with mass and coupling strength at the

electroweak scale have a relic density which is consistent with that of observed DM. In dense DM regions, the self-annihilation of WIMPs would give rise today to standard model particles, including a possible emission of very-high-energy (VHE,  $E_\gamma \gtrsim 100 \text{ GeV}$ )  $\gamma$  rays in the final state.

DM self-annihilations are expected to produce a continuum spectrum of  $\gamma$  rays up to the DM mass  $m_{\text{DM}}$  from prompt annihilation into quarks, heavy leptons or gauge bosons (a secondary emission from inverse Compton scattering and bremsstrahlung of electrons produced in the decay chain), and  $\gamma$ -ray lines. While the continuum signal is nontrivial to distinguish from other standard broadband astrophysical emissions, the DM self-annihilation at rest into  $\gamma X$  with  $X = \gamma, h, Z$  or a non-standard-model neutral particle would give a prominent and narrow spectral line at an energy  $E_\gamma = m_{\text{DM}}(1 - m_X^2/4m_{\text{DM}}^2)$ , limited only by the detector resolution given the low ( $\sim 10^{-3}c$ ) relative velocity of the DM particles. When DM self-annihilates into charged particles, additional  $\gamma$  rays are present from final state radiation and virtual internal bremsstrahlung. This produces bumpy bremsstrahlung features, giving a wider line that peaks at an energy near  $m_{\text{DM}}$  [6,7].

Since the DM is strongly constrained to be electrically neutral, the annihilation into monoenergetic  $\gamma$  rays is typically loop suppressed compared to the continuum signal, and the velocity-weighted annihilation cross section into two photons is about  $10^{-2} - 10^{-4}$  of the total velocity-weighted annihilation cross section  $\langle\sigma v\rangle$  (see, for instance, Refs. [8–11]). For WIMPs produced in a standard thermal history of the Universe,  $\langle\sigma v\rangle$  is about  $3 \times 10^{-26} \text{ cm}^3 \text{ s}^{-1}$  in order to reproduce the observed density of DM in the Universe [12]. VHE  $\gamma$ -ray lines can be detected by ground-based Cherenkov telescope arrays such as H.E.S.S. (High Energy Stereoscopic System).

The central region of the Galactic halo observed in VHE  $\gamma$  rays is among the most compelling targets to search for monoenergetic line signals from DM annihilations due to its proximity to Earth and predicted large DM concentration. For WIMPs in the TeV mass range, the strongest constraints so far reach  $\langle\sigma v\rangle \sim 3 \times 10^{-27} \text{ cm}^3 \text{ s}^{-1}$  at 1 TeV [13] using four years of observations of the Galactic center (GC) region with H.E.S.S.

The energy differential  $\gamma$ -ray flux produced by the annihilation of self-conjugate DM particles of mass  $m_{\text{DM}}$  in a solid angle  $\Delta\Omega$  can be written as

$$\frac{d\Phi}{dE_\gamma}(E_\gamma, \Delta\Omega) = \frac{\langle\sigma v\rangle}{8\pi m_{\text{DM}}^2} \frac{dN}{dE_\gamma}(E_\gamma) \times J(\Delta\Omega),$$

$$\text{with } J(\Delta\Omega) = \int_{\Delta\Omega} \int_{\text{LOS}} ds d\Omega \rho^2(r(s, \theta)). \quad (1)$$

The first term includes the DM particle physics properties.  $dN/dE_\gamma(E_\gamma) = 2\delta(m_{\text{DM}} - E_\gamma)$  is the differential  $\gamma$ -ray yield per annihilation into two photons.  $J(\Delta\Omega)$  denotes the integral of the square of the DM density  $\rho$  along the line of sight (LOS) in a solid angle  $\Delta\Omega$ . It is commonly referred to as the  $J$  factor [14]. The coordinate  $r$  is defined by  $r = (r_\odot^2 + s^2 - 2r_\odot s \cos\theta)^{1/2}$ , where  $s$  is the distance along the line of sight and  $\theta$  is the angle between the

direction of observation and the GC.  $r_\odot$  is the distance of the observer with respect to the GC, taken equal to 8.5 kpc [15]. In this work, we consider DM density distributions parametrized by cuspy profiles, for which archetypes are the Einasto [16] and Navarro-Frenk-White (NFW) [17] profiles (see also Ref. [18]). Cored profiles are not studied here, since they need specific data-taking and analysis procedures to be probed as shown in Ref. [19].

From ten years of observations of the GC region with the initial four telescopes of H.E.S.S., we present here a new search for DM annihilations into monoenergetic narrow  $\gamma$ -ray lines in the inner Galactic halo [13]. (We consider as a monoenergetic narrow line each structure that is narrow on the scale of the 10% energy resolution of H.E.S.S.) Exploiting the increased photon statistics, we perform the search in the mass range 300 GeV–70 TeV with an improved technique for  $\gamma$ -ray selection and reconstruction and a two-dimensional (2D) likelihood-based analysis method using the spectral and spatial features of the DM annihilation signal with respect to the background.

*Data analysis.*—The data set was obtained from GC observations with H.E.S.S. phase I during the years 2004–2014 as in Ref. [20] with telescope-pointing positions between  $0.5^\circ$  and  $1.5^\circ$  from the GC. Standard criteria for data quality selection are applied to the data to select  $\gamma$ -ray events [21]. In addition, observational zenith angles higher than  $50^\circ$  are excluded to minimize systematic uncertainties in the event reconstruction. The data set amounts to 254 h (live time) with a mean zenith angle of the selected observations of  $19^\circ$ . The  $\gamma$ -ray event selection and reconstruction make use of an advanced semianalytical shower model technique [22] in order to determine the direction and the energy of each event. With this technique, the energy resolution defined as the distribution of  $\Delta E/E = (E_{\text{reco}} - E_{\text{true}})/E_{\text{true}}$  has a rms of 10% above 300 GeV. This technique is also very well suited to mitigate the effects expected from the variations of the night sky background (NSB) in the field of view [22]. In the GC region, broad NSB variations may induce systematic effects in the event acceptance and, therefore, in the normalization of the signal and background region exposure [19,23]. A discussion on the systematic effects from NSB variations in the present analysis is given in Ref. [24].

The search for a DM signal is performed in regions of interest (ROIs) defined as annuli with inner radii of  $0.3^\circ$ – $0.9^\circ$  in radial distance from the GC, and a width of  $0.1^\circ$ , hereafter referred to as the on region. Following Ref. [20], a band of  $\pm 0.3^\circ$  along the Galactic plane is excluded to avoid astrophysical background contamination from the VHE sources such as HESS J1745-290 coincident in position with the supermassive black hole Sagittarius A\* [25,26], the supernova or pulsar wind nebula G0.9+0.1 [27], and a diffuse emission extending along the Galactic plane [28–30]. A disk with a  $0.4^\circ$  radius masks the supernova remnant HESS J1745-303 [31].

The background events are selected for each observation in an off region chosen symmetrically to the on region with respect to the observational pointing position. The on and off regions are thus taken with the same acceptance and observation conditions and have the same shape and solid angle size as shown in Fig. 1 in Supplemental Material [24]. Such a measurement technique enables an accurate background determination which does not require further acceptance correction. The off regions are always sufficiently far away from the on region to obtain a significant DM gradient between the on and off regions for cuspy DM profiles. For such profiles, we consider off regions which are expected to contain always fewer DM events than the on regions. Figure 1 shows an example of  $J$ -factor values in the on and off regions for ROI 2 and two specific telescope-pointing positions. For the pointing position  $P(0.89, 0.12)$ , a gradient of about 3.5 is obtained between the on and off regions. See Supplemental Material [24] for more details, which includes Ref. [32].

We perform a 2D binned Poisson maximum likelihood analysis in order to exploit the spatial and spectral characteristics of the DM signal with respect to the background. The energy range is divided into 60 logarithmically spaced bins between 300 GeV and 70 TeV. Seven spatial

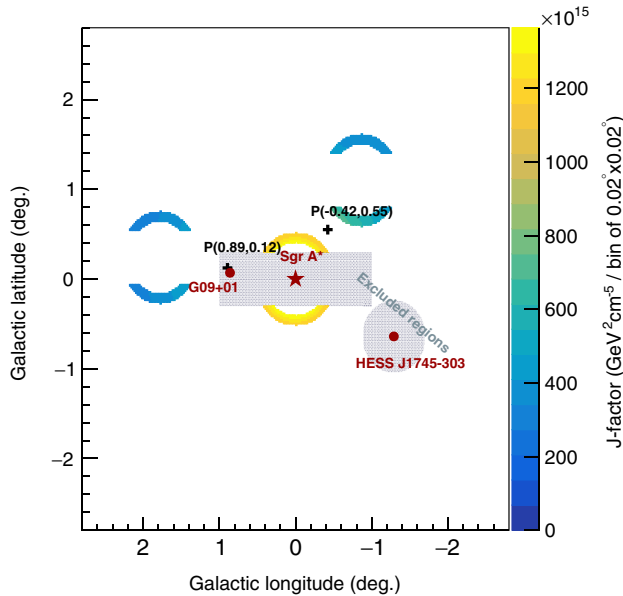


FIG. 1. Schematic of the background measurement technique for ROI 2 and two different telescope-pointing positions, in Galactic coordinates. The off region is taken symmetrically to the on region from a given observational pointing position (black cross). Two off regions are shown, each one corresponding to a specific pointing position. On and off regions have the same angular size and shape. The positions of Sgr A\* (red star), G0.9 + 0.1 (red dot), and HESS J1745-303 (red dot) are shown. The gray-filled box with Galactic latitudes from  $-0.3^\circ$  to  $+0.3^\circ$  and the gray-filled disk are excluded for signal and background measurements. The color scale gives the  $J$ -factor value per spatial bin of  $0.02^\circ \times 0.02^\circ$  for the Einasto DM profile.

bins corresponding to ROIs defined as the above-mentioned annuli of  $0.1^\circ$  width are chosen following Ref. [20]. For a given DM mass, the total likelihood function is obtained from the product of the individual Poisson likelihoods  $\mathcal{L}_{ij}$  over the spatial bins  $i$  and the energy bins  $j$ :

$$\begin{aligned} \mathcal{L}_{ij}(\mathbf{N}_{\text{on}}, \mathbf{N}_{\text{off}}, \alpha | \mathbf{N}_{\text{S}}, \mathbf{N}'_{\text{S}}, \mathbf{N}_{\text{B}}) \\ = \frac{(N_{S,ij} + N_{B,ij})^{N_{\text{on},ij}}}{N_{\text{on},ij}!} e^{-(N_{S,ij} + N_{B,ij})} \\ \times \frac{(N'_{S,ij} + \alpha_i N_{B,ij})^{N_{\text{off},ij}}}{N_{\text{off},ij}!} e^{-(N'_{S,ij} + \alpha_i N_{B,ij})}. \end{aligned} \quad (2)$$

For each bin  $(i, j)$ ,  $N_{\text{on}}$  and  $N_{\text{off}}$  are the measured number of events in the on and off regions, respectively.  $\alpha = \Delta\Omega_{\text{off}}/\Delta\Omega_{\text{on}}$  corresponds to the ratio of the solid angle sizes of the off and on regions. Here,  $\alpha_i = 1$  by definition of the on and off regions. The expected number of background events  $N_B$  in the on region is extracted from residual background measurements in the data set.  $N_S$  and  $N'_S$  stand for the number of signal events expected in the on and off regions, respectively. They are obtained by folding the theoretical number of DM events with the energy-dependent acceptance and energy resolution of H.E.S.S. for this data set. The  $\gamma$ -ray line signal is represented by a Gaussian function at the line energy  $E_\gamma = m_{\text{DM}}$  with a width of  $\sigma/E_\gamma$ . The vectors  $\mathbf{N}_{\text{on}}, \mathbf{N}_{\text{off}}, \mathbf{N}_{\text{S}}, \mathbf{N}'_{\text{S}}, \mathbf{N}_{\text{B}}$ , and  $\boldsymbol{\alpha}$  represent the lists of the corresponding quantities for all bins.

In the absence of statistically significant  $\gamma$ -ray excess in the on region with respect to the off region, constraints on the DM line flux and velocity-weighted annihilation cross section can be obtained from the likelihood ratio test statistic given by  $\text{TS} = -2 \ln[\mathcal{L}(m_{\text{DM}}, \langle\sigma v\rangle)/\mathcal{L}_{\text{max}}(m_{\text{DM}}, \langle\sigma v\rangle)]$ . In the high statistics limit, TS follows a  $\chi^2$  distribution with one degree of freedom [33]. Values of  $\Phi$  and  $\langle\sigma v\rangle$  for which the TS value is higher than 2.71 provide one-sided 95% confidence level (C.L.) upper limits on the flux and velocity-weighted annihilation cross section, respectively. Uncertainties in the energy reconstruction scale and the energy resolution affect these limits by less than 25%. The systematic uncertainty arising from NSB variations in the field of view modifies the limits up to 60%. See Ref. [24] for more details.

**Results.**—We find no statistically significant  $\gamma$ -ray excess in any of the ROIs with respect to the background. A cross-check analysis using independent event calibration and reconstruction [34] confirms the absence of any significant excess. We derive upper limits on  $\Phi$  and  $\langle\sigma v\rangle$  at 95% C.L. for DM masses from 300 GeV to 70 TeV. The left panel in Fig. 2 shows the observed upper limits at 95% C.L. on the flux from prompt DM self-annihilations into two photons for the Einasto profile. (Assuming a kiloparsec-sized cored DM density distribution such as the Burkert profile would weaken the limits by about 2–3 orders of magnitude.) In order to check that the observed limits are in agreement

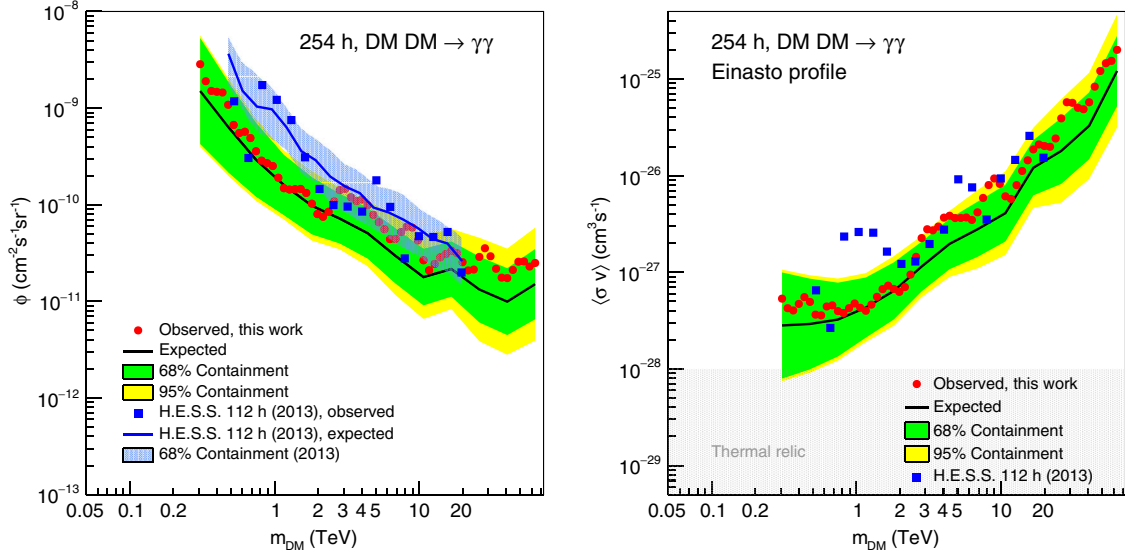


FIG. 2. Constraints on the flux  $\Phi$  (left panel) and on the velocity-weighted annihilation cross section  $\langle\sigma v\rangle$  (right panel) for the prompt annihilation into two photons derived from H.E.S.S. observations taken over ten years (254 h of live time) of the inner 300 pc of the GC region. The constraints are expressed in terms of 95% C.L. upper limits as a function of the DM mass  $m_{\text{DM}}$  for the Einasto profile. The observed limits are shown as red dots. Expected limits are computed from 1000 Poisson realizations of the expected background derived from blank-field observations at high Galactic latitudes. The mean expected limit (black solid line) together with the 68% (green band) and 95% (yellow band) C.L. containment bands are shown. The bands include the statistical and the systematic uncertainties. The observed limits derived in the analysis of four years (112 h of live time) of GC observations by H.E.S.S. [13] are shown as blue squares, together with the mean expected limit (blue solid line) and the 68% containment band (blue shaded area) in the left panel. The natural scale for monochromatic  $\gamma$ -ray line signal is highlighted as a gray-shaded area in the right panel.

with random fluctuations of the expected background, we computed expected limits using the likelihood ratio TS from 1000 Poisson realizations of the expected background derived from observations of blank fields at high latitudes where no signal is expected (see Supplemental Material [24]). For each DM mass, the mean expected upper limit and the 68% and 95% containment bands are extracted from the obtained  $\Phi$  and  $\langle\sigma v\rangle$  distributions and are plotted in the left panel in Fig. 2. In addition to the statistical uncertainty, the containment bands include the systematic uncertainties coming from the energy scale, the energy resolution, and NSB variations in the field of view [24].

We obtain the largest improvement in the observed flux limits compared to the previous results published in Ref. [13] for a DM particle mass of 1 TeV, where the limits are stronger by a factor of 6. The improved photon statistics, the likelihood analysis method using both on and off Poisson terms, and the 2D likelihood analysis method yield an increase of sensitivity by a factor of about 1.4, 1.8, and 1.3, respectively. The remaining improvement factor comes from the improved  $\gamma$ -ray event selection and reconstruction technique used in the present analysis [22]. The 95% C.L. observed flux limit reaches  $\sim 1.6 \times 10^{-10} \text{ cm}^{-2} \text{ s}^{-1} \text{ sr}^{-1}$  at 1 TeV. The right panel in Fig. 2 shows the 95% C.L. upper limits on  $\langle\sigma v\rangle$  for the Einasto profile, together with the natural scale for gamma-ray lines from thermal Higgsinos annihilating into two photons

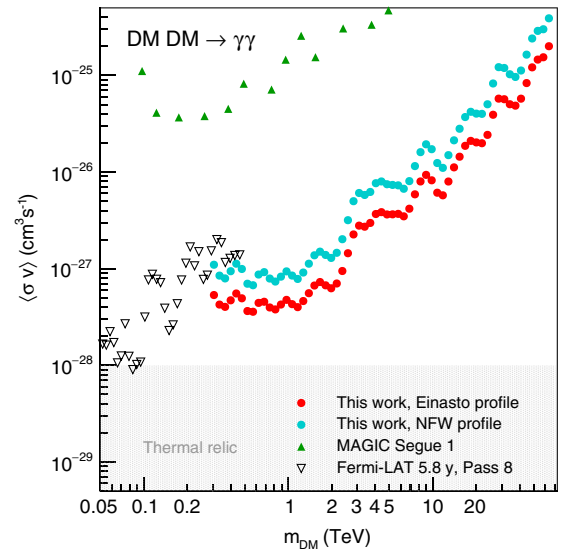


FIG. 3. Comparison of constraints for prompt annihilation into two photons obtained by H.E.S.S. for the Einasto (red dots) and NFW (cyan dots) profiles, with the limits from the observations of the Milky Way halo by Fermi-LAT [35] (black triangles) as well as the limits from 157 h of MAGIC observations of the dwarf galaxy Segue 1 [36] (green triangles). The gray-shaded area shows the natural scale for a monochromatic  $\gamma$ -ray line signal.

[8] and from final state radiation and internal bremsstrahlung [7].) The observed and the expected limits together with their 68% and 95% C.L. containment bands are plotted. For a DM particle of mass 1 TeV, the observed limit is  $\langle\sigma v\rangle \simeq 4 \times 10^{-28} \text{ cm}^3 \text{ s}^{-1}$ .

In Fig. 3, we show a comparison of our results with the current constraints on the prompt DM self-annihilation into two photons obtained from 5.8 years of observations of the Milky Way halo (the observed limits for Fermi-LAT are extracted for the DM density profile labeled as Einasto R16 in Ref. [35]) by the Fermi-LAT satellite [35] and the limits from 157 h of observations of the dwarf galaxy Segue 1 (the  $J$  factor of Segue 1 used in Ref. [36] could be overestimated by a factor of 100 as shown in Ref. [37]) by the MAGIC ground-based Cherenkov telescope instrument [36]. The previous limits obtained by H.E.S.S. from 112 h of observations of the GC [13] are also plotted.

*Summary and discussion.*—We presented a new search for monoenergetic VHE  $\gamma$ -ray lines from ten years of observation of the GC (254 h of live time) by phase I of H.E.S.S. with a novel statistical analysis technique using a 2D maximum likelihood method. No significant  $\gamma$ -ray excess is found, and we exclude a velocity-weighted annihilation cross section into two photons of  $4 \times 10^{-28} \text{ cm}^3 \text{ s}^{-1}$  for DM particles with a mass of 1 TeV for an Einasto profile. We obtain the strongest limits so far for DM masses above 300 GeV.

The limits obtained in this work significantly improve over the strongest constraints so far from 112 h of H.E.S.S. observations towards the GC region in the TeV mass range [13]. The new constraints cover a DM mass range from 300 GeV up to 70 TeV. They provide a significant mass range overlap with the Fermi-LAT constraints. They surpass the Fermi-LAT limits by a factor of about 4 for a DM mass of 300 GeV [35].

Despite the gain in sensitivity, our upper limits are still larger than the typical cross sections for thermal WIMPs at  $\langle\sigma v\rangle \sim 10^{-29} \text{ cm}^3 \text{ s}^{-1}$  expected for supersymmetric neutralinos [8]. However, there are several WIMP models which predict larger cross sections. While being not thermally produced, they still produce the right relic DM density. Among the wide class of heavy WIMP models, those with enhanced  $\gamma$ -ray lines (see, for instance, Ref. [38]) are, in general, strongly constrained by the results presented here. The present results can be applied to models with wider lines, while dedicated analyses taking into account the intrinsic line shapes are required. They include models with  $\gamma$ -ray boxes [39] and scalar [40] and Dirac [41] DM models, as well as the canonical Majorana DM triplet fermion known as the wino in supersymmetry [42].

The limits obtained by H.E.S.S. in this work are complementary to the ones obtained from direct detection and collider production (i.e., LHC) searches. While the latter ones are powerful techniques to look for DM of masses of up to about 100 GeV, the indirect detection with  $\gamma$

rays carried out with the Fermi-LAT satellite and ground-based Cherenkov telescopes is the most powerful approach to probe DM in the higher mass regime, as shown from several studies developed in the framework of the effective field theory [43] and, more recently, using the simplified-model approaches (see, for instance, Ref. [44]). Observations with ground-based Cherenkov telescopes such as H.E.S.S. are unique to probe multi-TeV DM through the detection of  $\gamma$ -ray lines.

The upcoming searches with H.E.S.S. towards the inner Galactic halo will exploit additional observations including the fifth telescope at the center of the array. Since 2014, a survey of the inner Galaxy has been carried out with the H.E.S.S. instrument focusing in the inner  $5^\circ$  of the GC. This survey will allow us to probe a larger source region of DM annihilations and alleviate the impact of the uncertainty of the DM distribution in the inner kiloparsec of the Milky Way on the sensitivity to DM annihilations. A limited data set ( $\sim 15$  h) of this survey using 2014 observations with the fifth telescope only was used to constrain the presence of a 130 GeV DM line in the vicinity of the GC [45]. Observations including the fifth telescope will allow us to probe DM lines down to 100 GeV. In addition, a higher fraction of stereo events in the energy range from 100 to several hundred GeV is expected from the increased number of stereo triggers between the fifth telescope and one of the recently upgraded smaller telescopes. Beyond the sensitivity improvement expected from increased photon statistics, the inner Galaxy survey will provide a larger fraction of photons in regions devoid of known standard astrophysical emissions and, therefore, of prime interest for DM searches. Within the next few years, DM searches with H.E.S.S. will enable an even more in-depth exploration of the WIMP paradigm for DM particles in the 100 GeV–10 TeV mass range.

The support of the Namibian authorities and of the University of Namibia in facilitating the construction and operation of H.E.S.S. is gratefully acknowledged, as is the support by the German Ministry for Education and Research (BMBF), the Max Planck Society, the German Research Foundation (DFG), the Alexander von Humboldt Foundation, the Deutsche Forschungsgemeinschaft, the French Ministry for Research, the CNRS-IN2P3 and the Astroparticle Interdisciplinary Programme of the CNRS, the United Kingdom Science and Technology Facilities Council (STFC), the IPNP of the Charles University, the Czech Science Foundation, the Polish National Science Centre, the South African Department of Science and Technology and National Research Foundation, the University of Namibia, the National Commission on Research, Science and Technology of Namibia (NCRST), the Innsbruck University, the Austrian Science Fund (FWF), and the Austrian Federal Ministry for Science, Research and Economy, the University of Adelaide and the Australian Research Council, the Japan

Society for the Promotion of Science and the University of Amsterdam. We appreciate the excellent work of the technical support staff in Berlin, Durham, Hamburg, Heidelberg, Palaiseau, Paris, Saclay, and Namibia in the construction and operation of the equipment. This work benefited from services provided by the H.E.S.S. Virtual Organisation, supported by the national resource providers of the EGI Federation. Part of this work was funded by EU FP7 Marie Curie Grant Agreement No. PIEF-GA-2012-332350.

\*Present address: The School of Physics, The University of New South Wales, Sydney, 2052, Australia.

†Corresponding authors.

contact.hess@hess-experiment.eu

\*Present address: Instituto de Física de São Carlos, Universidade de São Paulo, Avenida Trabalhador São-carlense, 400—CEP 13566-590, São Carlos, SP, Brazil.

- [1] R. Adam *et al.* (Planck Collaboration), *Astron. Astrophys.* **594**, A1 (2016).
- [2] G. Jungman, M. Kamionkowski, and K. Griest, *Phys. Rep.* **267**, 195 (1996).
- [3] L. Bergstrom, *Rep. Prog. Phys.* **63**, 793 (2000).
- [4] G. Bertone, D. Hooper, and J. Silk, *Phys. Rep.* **405**, 279 (2005).
- [5] J. L. Feng, *Annu. Rev. Astron. Astrophys.* **48**, 495 (2010).
- [6] L. Bergstrom, *Phys. Lett. B* **225**, 372 (1989).
- [7] T. Bringmann, L. Bergstrom, and J. Edsjo, *J. High Energy Phys.* **01** (2008) 049.
- [8] L. Bergstrom and P. Ullio, *Nucl. Phys.* **B504**, 27 (1997).
- [9] F. Ferrer, L. M. Krauss, and S. Profumo, *Phys. Rev. D* **74**, 115007 (2006).
- [10] M. Gustafsson, E. Lundstrom, L. Bergstrom, and J. Edsjo, *Phys. Rev. Lett.* **99**, 041301 (2007).
- [11] S. Profumo, *Phys. Rev. D* **78**, 023507 (2008).
- [12] G. Steigman, B. Dasgupta, and J. F. Beacom, *Phys. Rev. D* **86**, 023506 (2012).
- [13] A. Abramowski *et al.* (H.E.S.S. Collaboration), *Phys. Rev. Lett.* **110**, 041301 (2013).
- [14] L. Bergstrom, P. Ullio, and J. H. Buckley, *Astropart. Phys.* **9**, 137 (1998).
- [15] A. M. Ghez *et al.*, *Astrophys. J.* **689**, 1044 (2008).
- [16] V. Springel, S. D. M. White, C. S. Frenk, J. F. Navarro, A. Jenkins, M. Vogelsberger, J. Wang, A. Ludlow, and A. Helmi, *Nature (London)* **456**, 73 (2008).
- [17] J. F. Navarro, C. S. Frenk, and S. D. M. White, *Astrophys. J.* **490**, 493 (1997).
- [18] M. Cirelli, G. Corcella, A. Hektor, G. Hütsi, M. Kadastik, P. Panci, M. Raidal, F. Sala, and A. Strumia, *J. Cosmol. Astropart. Phys.* **03** (2011) 051.
- [19] A. Abramowski *et al.* (H.E.S.S. Collaboration), *Phys. Rev. Lett.* **114**, 081301 (2015).
- [20] H. Abdallah *et al.* (H.E.S.S. Collaboration), *Phys. Rev. Lett.* **117**, 111301 (2016).
- [21] F. Aharonian *et al.* (H.E.S.S. Collaboration), *Astron. Astrophys.* **457**, 899 (2006).
- [22] M. de Naurois and L. Rolland, *Astropart. Phys.* **32**, 231 (2009).
- [23] H. Dickinson and J. Conrad, *Astropart. Phys.* **41**, 17 (2013).
- [24] See Supplemental Material at <http://link.aps.org/supplemental/10.1103/PhysRevLett.120.201101> for more details on the observational data set at the Galactic center, the signal and background measurement technique, the expected limit computation together and a study of the systematic uncertainties. In addition, the dependency of the limits for different dark matter profiles is provided.
- [25] F. Aharonian *et al.* (H.E.S.S. Collaboration), *Astron. Astrophys.* **425**, L13 (2004).
- [26] F. Aharonian *et al.* (H.E.S.S. Collaboration), *Astron. Astrophys.* **503**, 817 (2009).
- [27] F. Aharonian *et al.* (H.E.S.S. Collaboration), *Astron. Astrophys.* **432**, L25 (2005).
- [28] F. Aharonian *et al.* (H.E.S.S. Collaboration), *Nature (London)* **439**, 695 (2006).
- [29] A. Abramowski *et al.* (H.E.S.S. Collaboration), *Phys. Rev. D* **90**, 122007 (2014).
- [30] A. Abramowski *et al.* (H.E.S.S. Collaboration), *Nature (London)* **531**, 476 (2016).
- [31] F. Aharonian (H.E.S.S. Collaboration), *Astron. Astrophys.* **483**, 509 (2008).
- [32] A. Abramowski *et al.* (H.E.S.S. Collaboration), *Phys. Rev. Lett.* **106**, 161301 (2011).
- [33] W. A. Rolke, A. M. Lopez, and J. Conrad, *Nucl. Instrum. Methods Phys. Res., Sect. A* **551**, 493 (2005).
- [34] R. D. Parsons and J. A. Hinton, *Astropart. Phys.* **56**, 26 (2014).
- [35] M. Ackermann *et al.* (Fermi-LAT Collaboration), *Phys. Rev. D* **91**, 122002 (2015).
- [36] J. Aleksić *et al.* (MAGIC Collaboration), *J. Cosmol. Astropart. Phys.* **02** (2014) 008.
- [37] V. Bonnivard *et al.*, *Mon. Not. R. Astron. Soc.* **453**, 849 (2015).
- [38] J. Hisano, S. Matsumoto, and M. M. Nojiri, *Phys. Rev. Lett.* **92**, 031303 (2004).
- [39] A. Ibarra, A. S. Lamperstorfer, S. Lpez-Gehler, M. Pato, and G. Bertone, *J. Cosmol. Astropart. Phys.* **09** (2015) 048; **06** (2016) E02.
- [40] F. Giacchino, A. Ibarra, L. Lopez Honorez, M. H. G. Tytgat, and S. Wild, *J. Cosmol. Astropart. Phys.* **02** (2016) 002.
- [41] M. Duerr, P. Fileviez Perez, and J. Smirnov, *Phys. Rev. D* **92**, 083521 (2015).
- [42] M. Baumgart, T. Cohen, I. Mould, N. L. Rodd, T. R. Slatyer, M. P. Solon, I. W. Stewart, and V. Vaidya, *J. High Energy Phys.* **03** (2018) 117.
- [43] E. Charles *et al.* (Fermi-LAT Collaboration), *Phys. Rep.* **636**, 1 (2016).
- [44] A. M. Sirunyan *et al.* (CMS Collaboration), *J. High Energy Phys.* **07** (2017) 014.
- [45] H. Abdalla *et al.* (H.E.S.S. Collaboration), *Phys. Rev. Lett.* **117**, 151302 (2016).